Journal of Magnetism and Magnetic Materials 426 (2017) 580–587

Contents lists available at ScienceDirect

Journal of Magnetism and Magnetic Materials

journal homepage: www.elsevier.com/locate/jmmm

Residual stress characterization of steel TIG welds by neutron diffraction and by residual magnetic stray field mappings

Robert Stegemann[a,*], Sandra Cabeza[a], Viktor Lyamkin[a], Giovanni Bruno[a], Andreas Pittner[a], Robert Wimpory[b], Mirko Boin[b], Marc Kreutzbruck[a,c]

[a] Bundesanstalt für Materialforschung und -prüfung (BAM), Unter den Eichen 87, 12200 Berlin, Germany
[b] HZB Helmholtz-Zentrum Berlin, Hahn-Meitner-Platz 1, 14109 Berlin, Germany
[c] IKT, University of Stuttgart, Pfaffenwaldring 32, 70569 Stuttgart, Germany

ARTICLE INFO

Keywords:
GMR
Magnetic stray field
Neutron diffraction
Residual stress
TIG-welding

ABSTRACT

The residual stress distribution of tungsten inert gas welded S235JRC+C plates was determined by means of neutron diffraction (ND). Large longitudinal residual stresses with maxima around 600 MPa were found. With these results as reference, the evaluation of residual stress with high spatial resolution GMR (giant magneto resistance) sensors was discussed. The experiments performed indicate a correlation between changes in residual stresses (ND) and the normal component of local residual magnetic stray fields (GMR). Spatial variations in the magnetic field strength perpendicular to the welds are in the order of the magnetic field of the earth.

1. Introduction

Weiss stated that a ferromagnetic material sufficiently below the Curie point is practically “always magnetized to saturation” [1]. If a ferromagnetic sample appears non-magnetic the individual domains are randomly oriented and compensate each another [1,2]. The magnetic polarization of a sample increases first when the magnetization vectors of domains are aligned in one direction due to external magnetic fields [1,3]. Simultaneously, the material can change its shape with magnetization – the so-called magnetostriction effect [4]. The relationship is also reciprocal: the magnetization of the sample changes when strained and is then called the Villari effect [5]. For small changes in magnetostriction or stress a thermodynamic relation can be established:

$$\left(\frac{1}{l}\frac{\partial l}{\partial H}\right)_{\sigma,T} = \left(\frac{\partial B}{\partial \sigma}\right)_{H,T} \quad (1)$$

between the change of induction **B** with stress $\boldsymbol{\sigma}$ and length l, as affected by field strength **H** at given temperature T. If magnetostriction $\frac{\Delta l}{l}$ is positive, **B** will increase by tension and decrease when magnetostriction is negative [3].

Aside from field strength and temperature, stress is a primary influence factor on the magnetic properties of ferromagnetic materials [3]. According to Becker [1], at ambient temperature and in the absence of a dominant external field, the spontaneous magnetization of domains in each small volume of a homogeneously strained ferromagnetic material adopts the direction of the maximum principal stress. Assuming that the absence of a dominant external field is in sufficient accuracy the magnetic field of the earth and the implicit understanding of the residual stresses are high enough to outbalance the influence of magnetocrystalline anisotropy [3,6,7], the magnetization direction is again dependent on the magnetostriction [1,3,6,8]. However, the presence of a weak external field is required: as long as no external magnetic field is acting, the parallel and anti-parallel orientations of domains are equivalent in terms of stress [8].

Although the direct magnetostriction effect is a structure-sensitive property, hence not a material constant [9], and small for common steels (a maximum value is typically given of the order of 10^{-6} [3,10,11]), the inverse effect is of particular significance for ferromagnetic material and highly sensitive to such properties as permeability μ and hysteresis loss. Eq. (1) merely shows that in materials with large magnetostrictive strain derivative $(\partial l/\partial H)_{\sigma,T}$ a large magnetomechanical effect $(\partial B/\partial \sigma)_{H,T}$ should be observed [12].

The physical coupling between mechanical stress and magnetization in ferromagnetic materials [3,12–14] can lead to the assumption that magnetic stray fields (SFs) close to the surface indicate zones of different magnetization. This, in turn, could correspond to the internal stress of the specimen [6,8,15]. Consequently, a relation is assumed between SF and (residual) stresses [16–22], or SF and local increase of

* Corresponding author.
E-mail address: Robert.Stegemann@bam.de (R. Stegemann).

http://dx.doi.org/10.1016/j.jmmm.2016.11.102
Received 26 July 2016; Received in revised form 28 October 2016; Accepted 21 November 2016
Available online 23 November 2016
0304-8853/

strain [23–25].

The objective of this paper is to discuss whether there is access to local change of homogeneous strained areas with sufficient high spatial resolution measurement equipment to evaluate the influence of (residual) stress on the (residual) magnetic field. For non-destructive testing (NDT) adapted giant magneto resistance (GMR) sensor arrays [26] provide high degree of spatial resolution due to the small size of their active layers. Although sensitivity of GMR probes are in general more than one order of magnitude below Fluxgate and SQUIDs, the application of these tiny sensors has an enormous advantage for the detection of fine spatial distributed and inhomogeneous magnetic fields, because small and local magnetic peaks are not averaged out by large sensing areas [27].

For quantitative residual stress state characterization, neutron diffraction (ND) is a well-known method, often used as a reference for (poly-) crystalline materials [28]. The penetration depth of neutrons into matter is superior to ionizing radiation, because the particles are uncharged and interact via nuclear forces. They are, therefore, particularly well-suited for NDT of bulky parts, including ones with difficult geometries [29]. The diffraction phenomenon occurs when a crystalline material is illuminated by a neutron beam with a wavelength λ comparable with the inter-planar lattice spacing d (Fig. 1) as a result of the reflection from crystal lattice planes hkl in Bragg condition

$$2d_{hkl}\sin(\theta_{hkl}) = n\lambda, \quad (2)$$

where n=1 and θ is the scattering angle of the incident beam, where the neutron detector should be placed. The nominal gauge volume is given by the intersection of the incident and diffracted beams, over which the strain measurement is averaged.

2. Experimental methodology

2.1. Material processing and characterization

The material under study is a commercial S235JRC+C (material no. 1.0120) low carbon structural steel cold drawn sheet with 5 mm thickness. The composition was analyzed by atomic emission spectroscopy with arc spark spectrometer Spectrotest (SPECTRO Analytical Instruments GmbH, Kleve, Germany), proving a hypoeutectoid carbon composition with small amounts of alloying elements and impurities under the tolerances (Si < 4%, P, S < 0.035%) – see Table 1. Four plates were sliced and ground alternately on both size to their final size of 250 × 100 × 4.8 mm^3, then demagnetized in a decreasing alternating field. Tungsten inert gas (TIG) welding without filler wire was carried out in the middle of the plates (see Fig. 2(a)) while the plates were fixed

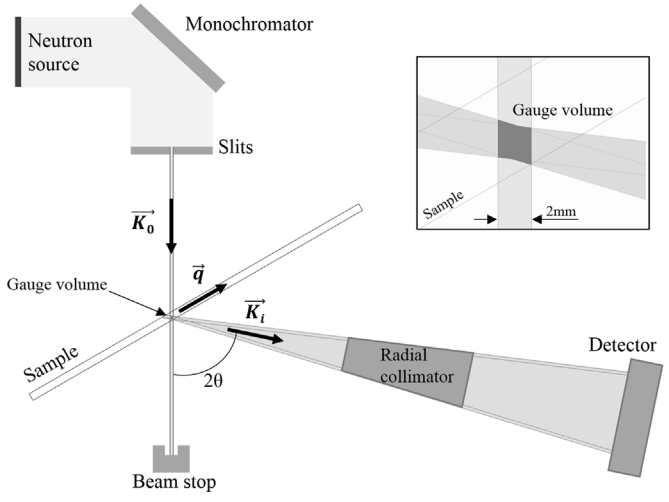

Fig. 1. Setup sketch of neutron diffraction (ND) measurements. K_0: incident beam, K_i: diffracted beam, q: scattering vector, 2θ: scattering angle for hkl diffraction.

Table 1
Chemical composition in weight percent (wt%).

C	Cu	Mn	Ni	Cr	Si	Al	P	S	Fe
0.065	0.47	0.41	0.16	0.13	0.23	0.05	0.02	0.01	BAL

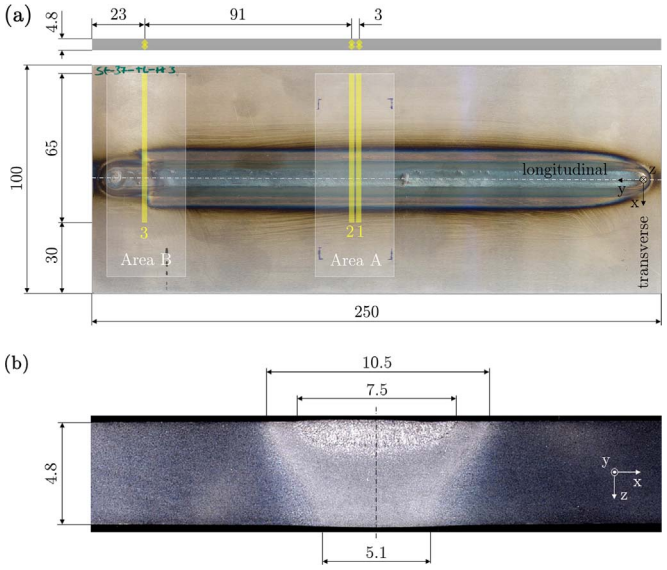

Fig. 2. (a) Photograph (top side) and dimensions (in millimeters) of presented welded specimen, position of the ND measuring zones are marked with yellow bars and the magnetic field mappings with transparent areas A and B. (b) Optical micrograph (Nital etching) of cross-section perpendicular to the weld (area A). (For interpretation of the references to color in this figure caption, the reader is referred to the web version of this paper.)

with clamps. The welding speed was set to 20 cm/min with 200 A of constant current (12.5 V). Filler wire was omitted to perform the welding as a local heat treatment (dummy welds/simulation welds) to minimize the change of chemical composition and topography. This resulted in a molten base material (fusion zone) close to the surface.

Internal stresses are generated during welding due to nonuniform heating, thermal contraction, solidification and different cooling rates [30]. The side of the plate with direct heat treatment is defined as “top”, the other side as “bottom” in the following. A micrograph of a cross-section slice transversal to the weld was prepared by grinding, polishing and Nital etching (Fig. 2(b)). The topography was analyzed by fringe projection (MicroCAD compact, GFMesstechnik GmbH, Teltow, Germany).

2.2. Neutron diffraction stress analysis

The residual strain characterization was conducted at the BERII reactor on the E3 instrument (Helmholtz-Zentrum Berlin, HZB). The Fe-211 ferrite peak was measured, considering a gauge volume of 2 × 2 × 2 mm^3 within the samples. Under the assumption that of a plane stress state due to the sample geometry, a point-wise mapping was performed along the principal stress directions being coincident with the transversal σ_{xx} and longitudinal σ_{yy} directions of welding (Fig. 2).

For the determination of the strain free lattice spacing (d^0_{hkl}) in different welding zones, a “comb” reference specimen with teeth 2 × 2 mm^2 in section was produced by electrical discharge machining (AP450 Sodick GmbH, Düsseldorf, Germany) using a wire diameter of 0.2 mm. This guaranteed the macro stress release throughout each cuboid [29,31]. Then the calculation of stresses was performed with their corresponding position in the strain free reference comb sample, allowing us to compensate for possible microstructural variations in